Supplemental Materials: Supplemental Figures and Legends, and Supplemental Tables for

"The evolutionarily conserved Arginyltransferase1 mediates a pVHL-independent oxygen-sensing pathway in mammalian cells"

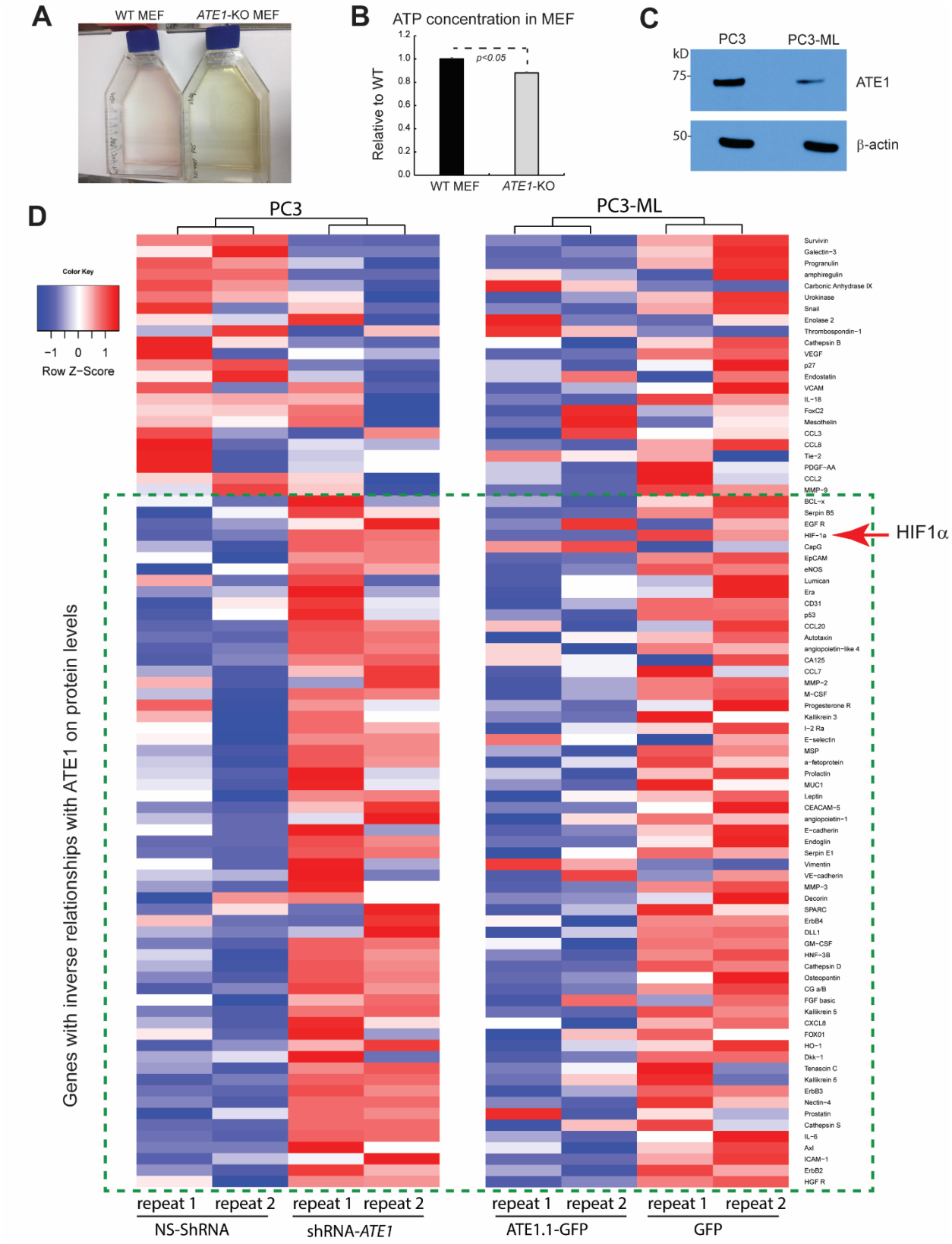

Supplemental Figure S1. Ate1 controls glycolysis by regulating HIF1α, related to Figure 1 and 2.

A) The color of culture media for actively growing WT and *ATE1*-KO MEF grown for two days. The cells were still sub-confluent. The media contains phenol red and yellow color indicates acidic pH.

B) Concentration of ATP in WT and *ATE1*-KO MEF measured by luciferase assay and normalized by cell number and average cell volume. The measurements were repeated 5 times (n=5) and the value of WT cells at one measurement was set as 1.0 and the other data were normalized to it.

C) The protein level of ATE1 in two human prostate cancer cell lines: PC3 and PC3-ML. PC3-ML is derived from PC3 but naturally has a lower ATE1 level and behaves much more aggressively in most cancer phenotypes[1]. In this case, the signal of the immunoblot was documented in the film while, elsewhere in this study, the acquisitions were done by a digital imaging platform.

D) Antibody array showing the changes of protein levels associated the manipulation of ATE1 levels. Considering that arginylation often induces degradation, we aimed to identify proteins whose levels are negatively correlated with ATE1 level. The downregulation of ATE1 was performed in human prostate cancer cell PC3 with specific shRNA in comparison to nonsilencing (NS) shRNA. The upregulation of ATE1 was accomplished with stable expression of GFP-fused mouse ATE1 isoform 1 (a ubiquitously expressed splice variant[2]) in PC3-ML by a moderate promoter at a level close to endogenous ATE1 as previously reported[3,4]. GFP was used as a control. An antibody array for 86 proteins commonly associated with metabolism and oncology was used to measure the changes of protein levels compared to the corresponding controls. The blue color indicates a reduction while red indicates an elevation. The box with a green dotted line indicates the proteins whose level is in an inverse relationship to ATE1 (i.e., increased in ATE1-downregulation and decreased with ATE1-upregulation). A red arrow indicates the position of HIF1α – one of the positive hits in this screening – showing an inverse correlation with ATE1 levels.

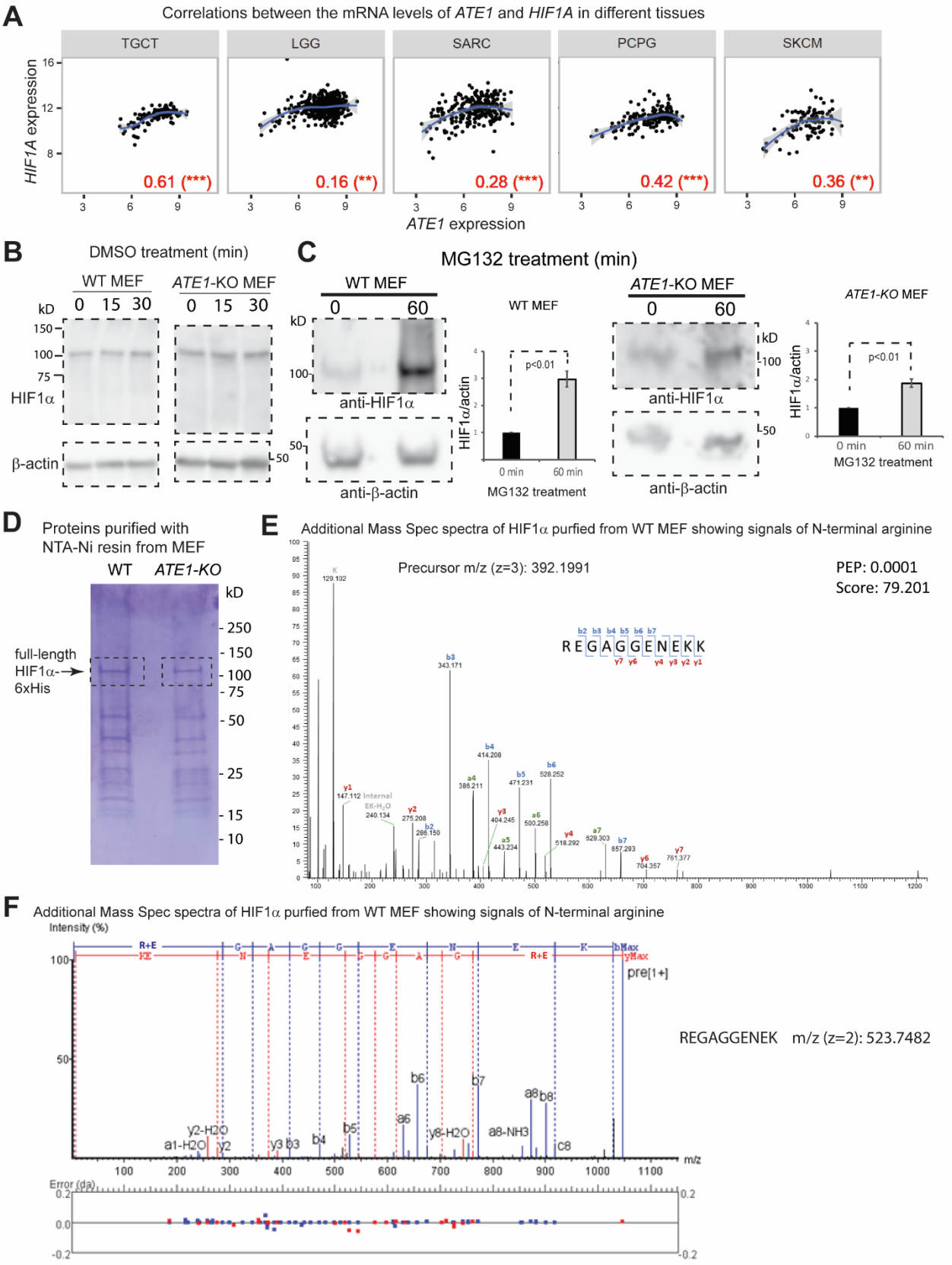
A
Correlations between the mRNA levels of ATE1 and HIF1A in different tissues
TGCT
LGG
SARC
PCPG
SKCM
HIF1A expression
ATE1 expression
0.61 (***)
0.16 (**)
0.28 (***)
0.42 (***)
0.36 (**)
B
DMSO treatment (min)
WT MEF
ATE1-KO MEF
0 15 30
kD
150
100
75
HIF1α
β-actin
C
MG132 treatment (min)
WT MEF
0 60
kD
100
anti-HIF1α
50
anti-β-actin
HIF1α/actin
p<0.01
0 min
60 min
MG132 treatment
ATE1-KO MEF
D
Proteins purified with NTA-Ni resin from MEF
WT
ATE1-KO
kD
250
150
100
75
50
25
15
10
full-length HIF1α-6xHis
E
Additional Mass Spec spectra of HIF1α purfied from WT MEF showing signals of N-terminal arginine
Precursor m/z (z=3): 392.1991
PEP: 0.0001
Score: 79.201
REGAGGENEKK
F
Additional Mass Spec spectra of HIF1α purfied from WT MEF showing signals of N-terminal arginine
Intensity (%)
pre[1+]
REGAGGENEK m/z (z=2): 523.7482
m/z
Error (da)

Supplemental Figure S2. **Characterization of HIF1α (mRNA and protein) and additional examples of mass spectrometry data showing the N-terminus arginylation of HIF1α, related to Figure 3 and 4.**

A) Graphs showing correlation of mRNA expression between *ATE1* and *HIF1A* genes in different tumor tissue collections in The Cancer Genome Atlas (TCGA) including: testicular germ cell tumors (TGCT), low-grade glioma (LGG), sarcoma (SARC), Pheochromocytoma and Paraganglioma (PCPG), and skin cutaneous melanoma (SKCM). The mRNA data (Pan-Cancer normalized RSEM values) were obtained from https://pancanatlas.xenahubs.net. Spearman's correlation coefficients were indicated in red fonts at the bottom of each plot. The number of tissue samples for each type of tumor were: TGCT: 134; LGG: 515; SARC: 259; PCPG: 179; SKCM: 103. The significance (p-value) was assessed for each analysis and shown in parentheses. The symbols *, **, and *** indicate p-values of <0.05, <0.005, and <0.0005, respectively.

B) Representative immunoblots showing the levels of HIF1α in WT and ATE1-KO MEF treated with DMSO over a time course as a reagent control for the cycloheximide treatment (Fig. 4B). The β-actin is a loading control.

C) Representative immunoblots and the corresponding quantifications (n=3) showing the HIF1α level, with β-actin as a loading control, in WT and ATE1-KO MEF treated with proteasome inhibitor MG132 for 1 hour. The short duration of the MG132 treatment is intended to minimize potential impacts from transcriptional changes.

D) A representative image of SDS-PAGE stained with Coomassie blue for proteins purified by NTA-Ni resin from WT and *ATE1*-KO MEF expressing recombinant mouse HIF1α fused with a C-terminal 6xHis tag. The boxes with the dotted line highlights the gel areas for the anticipated size of the full-length HIF1α-6xHis, which were cut and submitted separately for analysis by Mass Spectrometry.

E) In addition to the peptide sequence corresponding to REGAGENEK (shown in Fig 4C), we also detected peptide peaks corresponding to REGAGENEKK, which is a predicted alternative cleavage pattern of trypsin in arginylated HIF1α. The shown example is obtained from the proteomics core facility in USF, in which the submitted sample (SDS-PAGE slice) was analyzed within 2 days. The assignment of the b-ions (blue) and y-ions (red), as well as the PEP and Andromeda scores are indicated on the spectra.

F) An example of detected peptide peaks corresponding to REGAGENEK from the predicted arginylated N-terminus of HIF1α, obtained from the laboratory of Dr. Aldrin Gomes at the University of California, Davis. The mass of arginine (R) is predicted as 156.10. The assignment of b-ions (blue) and y-ions (red) are indicated on the spectra. The fragment error tolerance for the arginylated peptides was < 0.05 daltons. In this facility, the submitted samples (SDS-PAGE slices) were analyzed within one week.

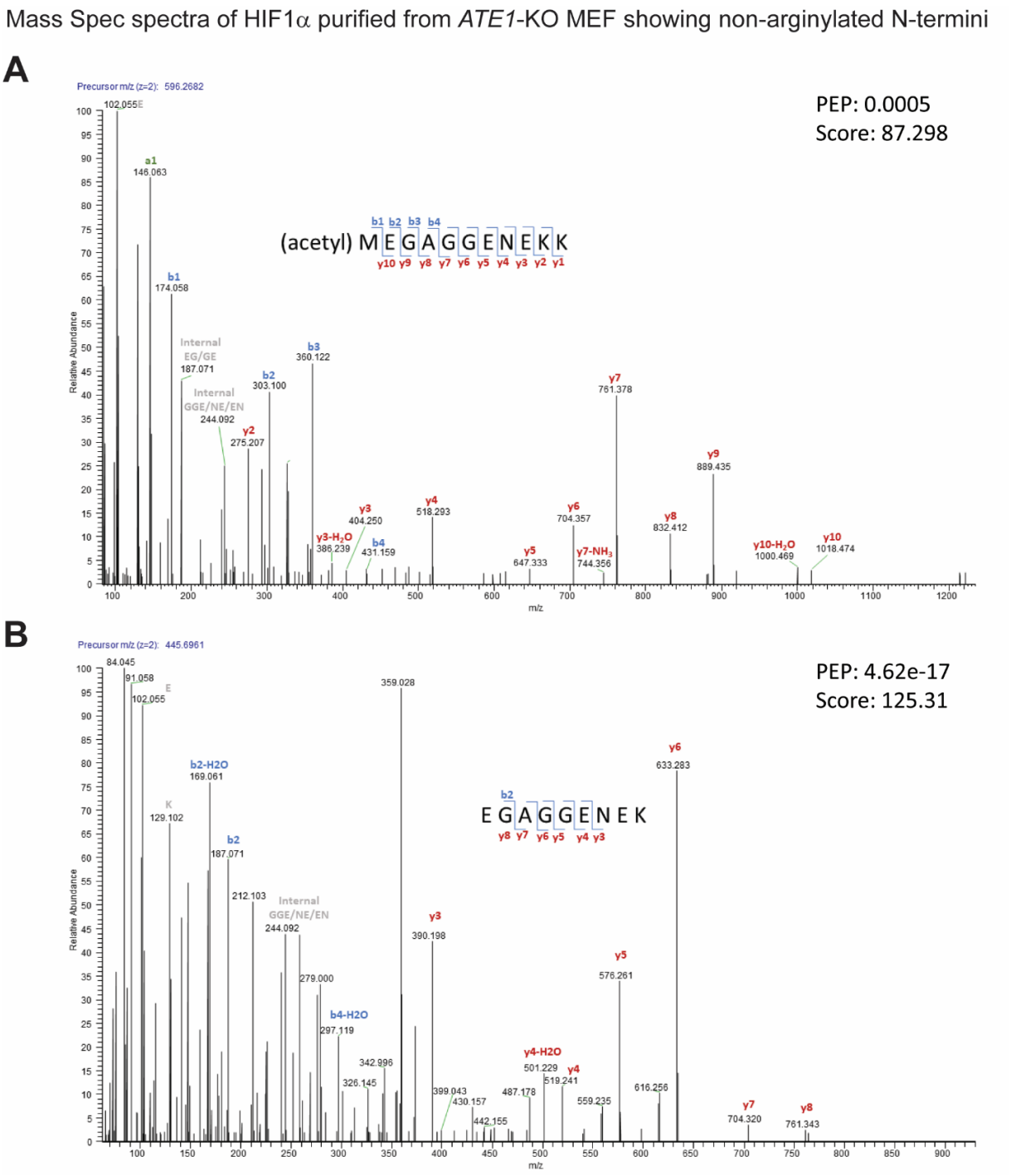

Supplemental Figure S3. Examples of Mass Spec results on HIF1α purified from *ATE1*-KO MEF showing peptide peaks of the non-arginylated N-terminus, related to Figure 4.

In HIF1α purified from arginylation-deficient *ATE1*-KO MEF, we did not detect any peptide peaks corresponding to N-terminal arginylated HIF1α. The two displayed examples are both acquired in the proteomics core facility of USF, in which the samples were analyzed within 2 days. In **A)**, a spectrum corresponding to N-terminal acetylated HIF1α is shown. In **B)**, a spectrum corresponding to the N-terminal sequence of HIF1α, after the initial methionine is removed, is shown. The assigned b-ions (blue) and y-ions (red), as well as the PEP and Andromeda scores are indicated.

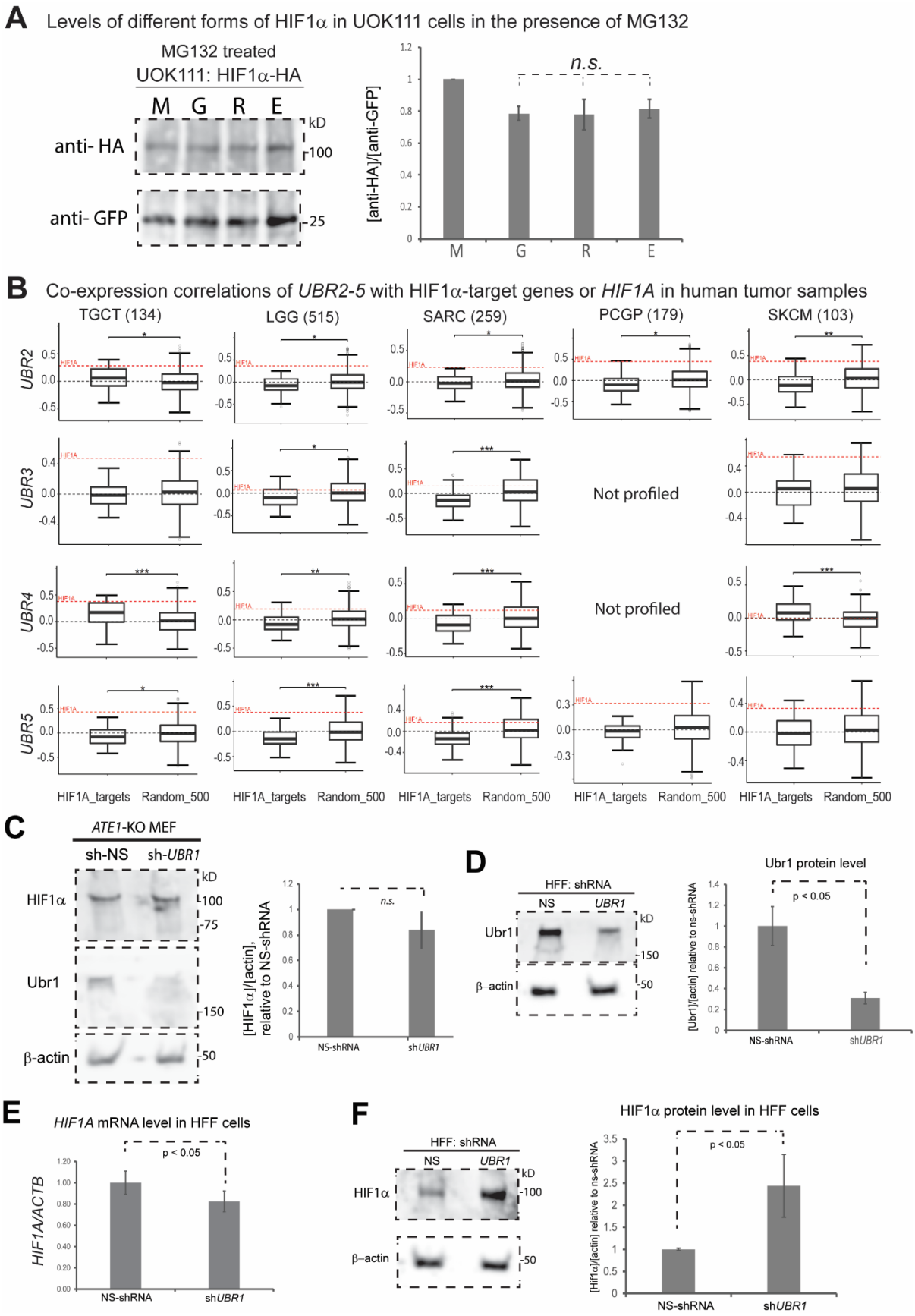
A
Levels of different forms of HIF1α in UOK111 cells in the presence of MG132
MG132 treated
UOK111: HIF1α-HA
M G R E
anti- HA
anti- GFP
kD
100
25
n.s.
[anti-HA]/[anti-GFP]
B
Co-expression correlations of UBR2-5 with HIF1α-target genes or HIF1A in human tumor samples
TGCT (134)
LGG (515)
SARC (259)
PCGP (179)
SKCM (103)
UBR2
UBR3
UBR4
UBR5
Not profiled
HIF1A_targets
Random_500
C
ATE1-KO MEF
sh-NS
sh-UBR1
HIF1α
Ubr1
β-actin
kD
100
75
150
50
n.s.
[HIF1α]/[actin], relative to NS-shRNA
NS-shRNA
shUBR1
D
HFF: shRNA
NS
UBR1
Ubr1
β–actin
kD
150
50
Ubr1 protein level
p < 0.05
[Ubr1]/[actin] relative to ns-shRNA
NS-shRNA
shUBR1
E
HIF1A mRNA level in HFF cells
p < 0.05
HIF1A/ACTB
NS-shRNA
shUBR1
F
HFF: shRNA
NS
UBR1
HIF1α
β–actin
kD
100
50
HIF1α protein level in HFF cells
p < 0.05
[Hif1α]/[actin] relative to ns-shRNA
NS-shRNA
shUBR1

Supplemental Figure S4. Additional evidence showing the relationship between UBRs and HIF1α, related to Figure 5.

A) Left: steady-state levels of recombinant HIF1α expressed in the pVHL-deficient human renal carcinoma cell line UOK111, after treatment of proteasome inhibitor MG132 for 3 hours. The different recombinant HIF1α include the non-arginylated (M-), arginylation-retarding (G-), constitutively arginylated (R-), or arginylation-eligible (E-) forms. Antibody against HA tag was used to detect the level of HIF1α while the level of GFP is used as loading controls to normalize the difference in expression efficiency of the vector. Right: the graph showing the quantification (n=3).

B) Coexpression correlations of *UBR2-5* with 50 HIF1A target genes in human tumor tissues. These samples include testicular germ cell tumors (TGCT), low-grade glioma (LGG), sarcoma (SARC), Pheochromocytoma, and Paraganglioma (PCPG), and skin cutaneous melanoma (SKCM) in The Cancer Genome Atlas (TCGA). The number of tissue samples for each type of tumor were indicated in the parenthesis. Note that not all genes were available from all tumor types in these databases. The mRNA data were Pan-Cancer normalized and obtained from https://pancanatlas.xenahubs.net. Spearman's correlation was used to calculate the co-expression correlation between *ATE1* and 50 HIF1α-target genes or a random set of 500 genes (Random-500, similarly as done in published studies[8-10]). The significance (p-value) was calculated by Mann−Whitney U test. The signs *, **, and *** indicate p-values of <0.05, <0.005, and <0.0005, respectively. See also Suppl. Table S1 for the list of the 50 HIF1α target genes that are known to be transcriptionally activated by HIF1α to be used for this co-expression analysis.

C) Representative immunoblots (left) showing the level of HIF1α with β-actin as loading control in *ATE1*-KO cells with *UBR1* knockdown, in comparison to non-silencing (NS) shRNA. The quantification on the right was based on three repeats (n=3).

D) Representative immunoblots and quantification based on five repeats (n=5) showing the knockdown efficiency of *UBR1* in HFF cells treated with non-silencing (ns) shRNA or specific shRNA against *UBR1*. The β-actin was used as a loading control.

E) The mRNA levels of HIF1A in HFF cells stably expressing non-silencing (ns) shRNA or shRNA against *UBR1*, measured by quantitative PCR. The human β-actin gene (ACTB) was used as a housekeeping gene for normalization. The quantification was based on two independent experiments with triplicates (n=3).

F) Representative images of an immunoblot showing the steady-state protein levels of HIF1α in HFF cells with non-silencing (ns) shRNA or specific shRNA against *UBR1* (sh*UBR1*). The β-actin was used as a loading control. The quantification shown on the right side was calculated from four independent repeats (n=4). Error bars represent SEM.

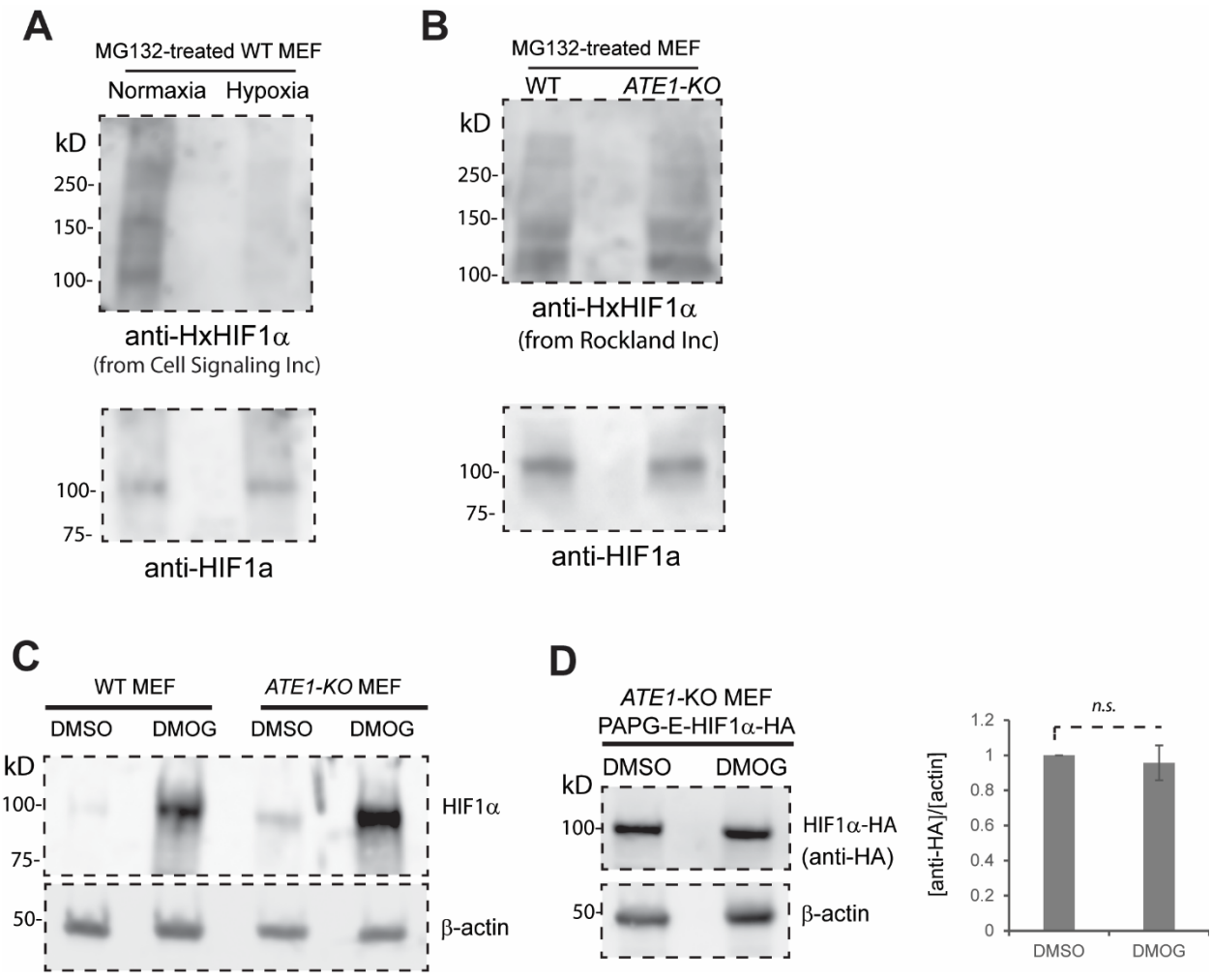

Supplemental Figure S5. The signal of hydroxylated-HIF1α and total HIF1α under different conditions, related to Figure 6

A) As a validation to the specificity of the anti-hydroxylated(Hx) HIF1α (from Cell Signaling Inc) as shown in Fig. 6C, an immunoblot showing the detection signals of this antibody in WT MEF incubated under normoxia or hypoxia (0.5% O_2) and treated with MG132 for 9 hours. To facilitate the specific comparison of the hydroxylation level of HIF1α, the loading of these samples was adjusted so that the two samples have comparable loading amounts of full-length HIF1α (probed by anti-HIF1α). As demonstrated by the immunoblots, the concerned anti-HxHIF1α antibody showed reduced signal with cells that were incubated with hypoxia – a condition expected to minimize the hydroxylation of HIF1α.

B) Immunoblots showing the levels of Hx-HIF1α, probed with rabbit HIF1α hydroxyl-P564(human)/P577(mouse) antibody (Rockland, Limerick, PA, Cat# 100-401-A25), in WT and *ATE1*-KO MEF treated with proteasome inhibitor MG132 (20μM) for 6 hours. The level of full-length HIF1α shown in the bottom, probed with anti-HIF1α, was pre-adjusted by the rationales as mentioned in (A).

C) Immunoblots showing the levels of endogenous HIF1α (with β-actin as loading controls) in WT and *ATE1*-KO MEF, treated with PHD inhibitor DMOG (20μM) for 6 hours. DMSO was used as a reagent control.

D) On the left are representative Immunoblots showing the levels of recombinant E-HIF1α fused with a C-terminal HA tag and carrying the PAPG mutations to the two critical proline residues (as described in

Fig.5A). This protein was stably expressed in arginylation-deficient *ATE1*-KO MEF, which were treated with PHD inhibitor DMOG (20μM), or the reagent control DMSO, for 6 hours. The level of the recombinant HIF1α was probed with anti-HA. The level of β-actin was used as a loading control. On the right is the quantification of the level of E-HIF1α-HA (n=3).

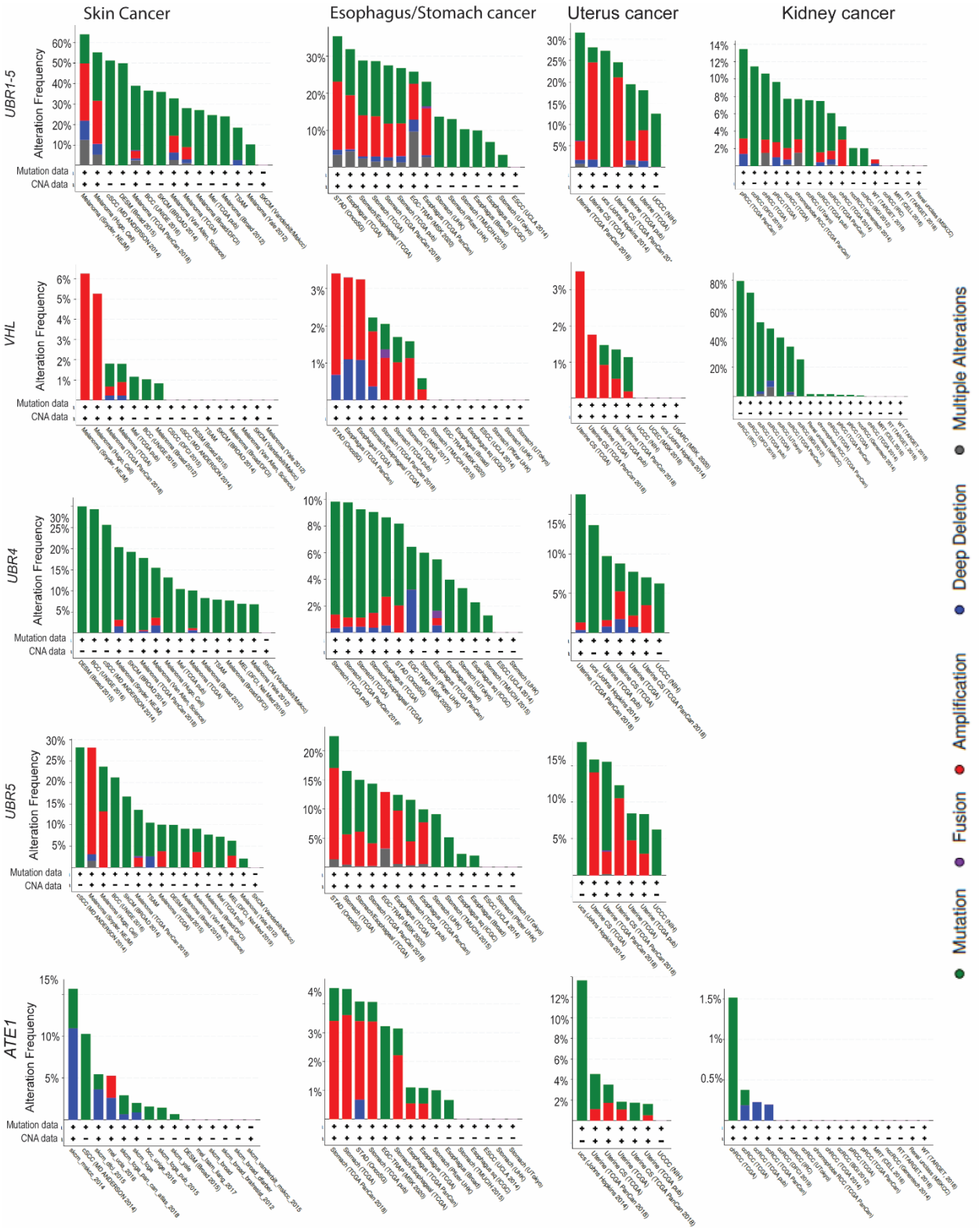

Supplemental Figure S6. Mutation burden on *UBR1-5, VHL and ATE1* in different types of solid tumors, related to Figure 5. The mutation burdens were analyzed by specific gene queries in cBioPortal for Cancer Genomics (https://www.cbioportal.org/), which contains genomic sequencing data from multiple published sources. The results are separated by cancer studies. The data corresponding to the skin,

esophagus/stomach, uterus and kidney cancer are shown as examples. In most examined cases, collective mutation burdens in the five *UBR* family genes (*UBR1-5*) are nearly 10-fold higher than *VHL*. Particularly, individual mutation burdens in *UBR4* or *UBR5* are 3-5 folds higher than in *VHL*.

The mutation burdens in *ATE1* is still higher than *VHL* in most cases, albeit lower than the *UBR* genes. This discrepancy may be explained by the "moonlighting" function of ATE1 in mitochondria[11], which is likely separate from its role in mediating protein degradation through the ubiquitin-proteasome system. Considering that mitochondrial functions are essential for certain types of cancer[12], this may become a limiting factor for mutations on *ATE1*.

Only in kidney cancer, we observed a higher mutation burden on *VHL* than *UBRs* or *ATE1*.

A Essential regions of HIF1α-like protein, NCBI accession no. XP_011403284.1 [Amphimedon queenslandica (sponge)], compared with human HIF1α protein (UniProtKB - Q16665)

```
XP_011403284.1    1    MEPSNRFDTTEPYSVLNRKERSRELAQKRRTTYKGLMKDLADELPFSKDVVSQVDYNSRLRLALCF
Q16665_hHIF1A     1    MEGAGGANDKKKISSERRKEKSRDAARSRRSKESEVFYELAHQLPLPHNVSSHLDKASVMRLTISY

cons                   ** :.  : .:  *  .***:**: *:.**:. . :: :**.:**:.::* *::*  * :**::.:
                  ...

XP_011403284.1    358  TPSVESSRSHDP----------------------------------------FPVPRDDGKSMDP
Q16665_hHIF1A     383  TSSLFDKLKKEPDALTLLAPAAGDTIISLDFGSNDTETDDQQLEEVPLYNDVMLPSPNEKLQNINL

                       *.*: .. . :*                                        :* *.:. :.::

                  ...

XP_011403284.1    556  TPTAVSPTPSFAESGITT------------DYGTYSPQISEEGFIKHELLSPTF-----------
Q16665_hHIF1A     512  EPNSPSEYCFYVDSDMVNEFKLELVEKLFAEDTEAKNPFSTQDTDLDLEMLAPYIPMDDDFQLRSF

cons                    *.: *    :.:*.:..            *  : .*  :::  :. *:*:* :
```

B Essential regions of HIF1α-like protein, NCBI Reference Sequence: XP_023346906.1 [Eurytemora affinis (Copepods)] compared with human HIF1α protein (UniProtKB - Q16665)

```
XP_023346906.1    1    MCGGVAGAQEPSQRFLKEFLKGSKRKRINSLEGLDGKAENQQEIQDLGALQQDNRKEKSRDAARNR
Q16665_hHIF1A     1    MEGG-A-------------------------------------NDKKKISSERRKEKSRDAARSR

cons                   *&** *                                    :*   :.:.:**********.*

                  ...

XP_023346906.1    403  DMGVDETFNLENPENMNEILEMLEQDAEELKMMDEEK------------KVKEELEKMEEVEKVEL
Q16665_hHIF1A     368  DMKMTQLFTKVESEDTSSLFDKLKKEPDALTLLAPAAGDTIISLDFGSNDTETDDQQLEEVPLYND

cons                   ** : : *.  :.*: ..::: *::::.: *.::                ..: : :::***   :

                  ...

XP_023346906.1    555  -------LGTGRRLSSDLENLSPFIGDECVPLNKTETLFQPLNL-----------------DSFDD
Q16665_hHIF1A     542  EDTEAKNPFSTQDTDLDLEMLAPYIPMDDDFQLRSFDQLSPLESSSASPESASPQSTVTVFQQTQI

cons                        : :  . *** *:*:*  :     ::   :.**:                  :. :
```

C HIF2α levels in WT and *ATE1*-KO MEF

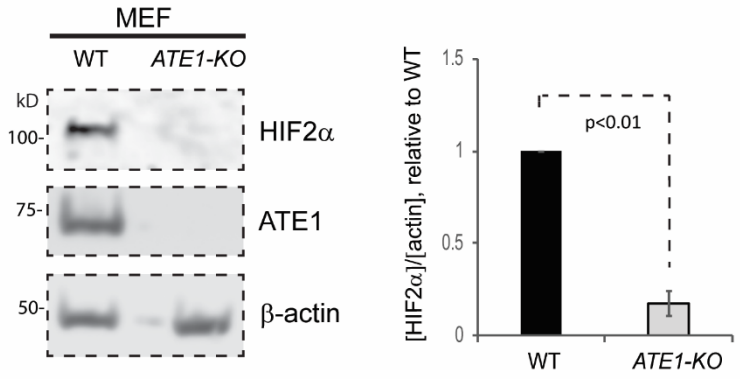

Supplemental Figure S7. Sequence alignment of HIF1α-like proteins in different species, and expression level of HIF2α in WT and *ATE1*-KO MEF, related to Figure 7

A) and **B)** Representative HIF1α-like proteins in sponge (A) and Copepods (B), compared with canonical HIF1α (UniprotKB – Q16665, human). Three segments are shown: the N-terminus and the two regions corresponding to the pVHL recognition sites in human HIF1α. The pink boxes indicate arginylation-eligible residues (D, E, N, Q, or C) at the 2nd residue of the N-terminus. The blue and the green box highlight the locations of the hydroxylation-eligible proline residue (P402 and P564) in human HIF1α. Both HIF1α-like proteins appear to have arginylation-eligible residues (D/E/N/Q/C) on the N-terminus, but only one hydroxylation-eligible proline (corresponding to P564 in human HIF1α). The signs "*", ":", and "." Indicates high to low consensus (cons). The sign "&" indicates Cysteine (C) on the N-terminus, which can be oxidized or nitrosylated to mimic an acidic residue[13,14].

No proteins containing the conserved functional domain (Pfam ID: 17211) of pVHL was found in Protista (Naegleria gruberi as example), Porifera (Amphimedon queenslandica), or Copepods (Eurytemora affinis) by searching the phylogenetic tree generated by pfam.xfam.org, or by performing BLASTp with the VHL-C domain or the full-length human pVHL (UniProtKB- P40337) at blast.ncbi.nlm.nih.gov with specific taxonomy. The presence of VHL-like protein was speculated in two species within the Porifera class Demosponges (Stylissa – taxid 237127 and Scopalina – taxid 85794)[15]. However, we did not find any meaningful match upon performing BLASTp by using the queries of VHL beta domain (Pfam ID: 01847), VHL box domain (Pfam ID: 17211), or full-length protein of human pVHL in these species.

(C) Representative immunoblots (left) and corresponding quantification graph (right, n=3) showing the levels of HIF2α in WT and *ATE1*-KO MEF with β-actin as loading controls.

Supplemental materials: Tables, Figures and Legends

Supplemental Table S1. 50 genes whose transcriptions are known to be activated by HIF1α			
Symbol	**Synonyms**	**Reference**	**regulation by HIF1α**
ABCB1	PGY1, ABC20, MDR1, GP170, CLCS, PGP, CD243, MGC163296	PubMed ID: 12067980	up-regulation
ABCG2	BCRP1, ABC15, MRX, MGC102821, EST157481, MXR, CD338, BCRP, ABCP, CDW338, MXR1, BMDP	PubMed ID: 15044468	up-regulation
ADM	AM	PubMed ID: 13130303	up-regulation
ALDOA	MGC17767, MGC17716, ALDA, MGC10942	PubMed ID: 8955077	up-regulation
CTSD	CPSD, MGC2311, CLN10	PubMed ID: 13130303	up-regulation
ENG	FLJ41744, END, CD105, ORW, ORW1, HHT1	PubMed ID: 12228247	up-regulation
ENO1	MBP1, MPB1, NNE, PPH, ENO1L1	PubMed ID: 8955077	up-regulation
EPO	EP, MGC138142	PubMed ID: 8408001	up-regulation
FN1	DKFZP686I1370, DKFZP686F10164, CIG, DKFZP686H0342, FNZ, EDB, LETS, DKFZP686O13149, MSF, GFND2, FINC, FN	PubMed ID: 13130303	up-regulation
GAPDH	MGC88685, GAPD, G3PD	PubMed ID: 10542317	up-regulation
HK1	HK1TA, HKI, HK1TC, HK1TB, HXK1	PubMed ID: 13130303	up-regulation
HK2	DKFZP686M1669, HKII, HXK2	PubMed ID: 13130303	up-regulation
IGF2	FLJ22066, INSIGF, C11ORF43, FLJ44734, PP9974	PubMed ID: 13130303	up-regulation
IGFBP1	IGFBP25, HIGFBP1, AFBP, IBP1, PP12	PubMed ID: 9707622	up-regulation
IGFBP2	IGFBP53, IBP2	PubMed ID: 13130303	up-regulation
IGFBP3	BP53, IBP3	PubMed ID: 13130303	up-regulation
KRT18	K18, CYK18	PubMed ID: 13130303	up-regulation
KRT19	CK19, MGC15366, K19, K1CS	PubMed ID: 13130303	up-regulation
LDHA	LDHM, PIG19, LDH1	PubMed ID: 13130303	up-regulation
LEP	FLJ94114, OB, OBS	PubMed ID: 12215445	up-regulation
MMP2	CLG4, CLG4A, TBE1, MMPII, MONA	PubMed ID: 13130303	up-regulation
NOS2A	NOS2, INOS, NOS, HEPNOS	PubMed ID: 13130303	up-regulation
PFKFB3	IPFK2, PFK2	PubMed ID: 15466858	up-regulation
PFKL	FLJ30173, FLJ40909, DKFZP686L2097, DKFZP686G1648, PFKB	PubMed ID: 13130303	up-regulation
PGK1	MGC142128, MGC117307, PGKA, MGC8947, MIG10	PubMed ID: 8955077	up-regulation

SERPINE1	PAI, PAI1, PLANH1	PubMed ID: 11877282	up-regulation
TGFA	TFGA	PubMed ID: 13130303	up-regulation
TGFB3	FLJ16571, TGFBETA3, ARVD	PubMed ID: 15155569	up-regulation
TPI1	MGC88108, TPI	PubMed ID: 13130303	up-regulation
VEGFA	MGC70609, VEGFA, VEGF, VPF	PubMed ID: 8756616	up-regulation
VIM	FLJ36605	PubMed ID: 13130303	up-regulation
EGLN1	HPH2, DKFZP761F179, ZMYND6, C1ORF12, PHD2, HIFPH2, SM20, ECYT3	PubMed ID: 15563275	up-regulation
EGLN3	FLJ21620, HIFPH3, MGC125999, PHD3, MGC125998	PubMed ID: 15823097	up-regulation
BNIP3	NIP3	PubMed ID: 12879018	up-regulation
CTGF	IGFBP8, MGC102839, HCS24, CCN2, NOV2	PubMed ID: 15315937	up-regulation
FURIN	PACE, FUR, SPC1, PCSK3	PubMed ID: 15611046	up-regulation
GPX3	GSHPXP, GPXP, GSHPX3	PubMed ID: 15096516	up-regulation
HSP90B1	GP96, GRP94, TRA1, ECGP	PubMed ID: 15620698	up-regulation
MET	HGFR, RCCP2, AUTS9	PubMed ID: 12726861	up-regulation
PDK1		PubMed ID: 16517405	up-regulation
SLC2A1	MGC141895, GLUT, MGC141896, GLUT1	PubMed ID: 13130303	up-regulation
TF	DKFZP781D0156, PRO1557, PRO2086	PubMed ID: 9242677	up-regulation
CXCL12	SDF1B, SDF1A, TPAR1, SDF1, TLSFA, TLSFB, PBSF, SCYB12	PubMed ID: 15235597	up-regulation
CXCR4	LCR1, NPYY3R, WHIM, HM89, LAP3, NPYRL, FB22, D2S201E, NPYR, NPY3R, LESTR, HSY3RR, CD184	PubMed ID: 13679920	up-regulation
CA9	MN, CAIX	PubMed ID: 15184875	up-regulation
FECH	FCE, EPP	PubMed ID: 15312748	up-regulation
MCL1	MCL1S, MGC104264, TM, MGC1839, MCL1L, EAT	PubMed ID: 15611089	up-regulation
MXI1	MGC43220, MAD2, MXD2, MXI	PubMed ID: 17482131	up-regulation
PDGFA	PDGF1, PDGFA	PubMed ID: 15132980	up-regulation
CYP2S1		PubMed ID: 17277313	up-regulation

Supplemental Table S1. The list of the 50 genes used as direct HIF1α-activating targets in this study, related to Figure 3.

These include genes that were demonstrated with experimental data for their transcription activation by HIF1α, and genes that are upregulated under hypoxic conditions and are predicted to bind HIF1α in their promoter regions. The table is adapted from published studies[5,6].

Supplemental Table S2. Oligonucleotides used in this study, related to STAR Methods and the Key Resources Table

Oligo name	Sequence
Hif1-NotI-F	ATTGATCCGCGGCCGCatggagggcgccggcggcgagaacgagaag
Hif1-BamH-6HIS-EcoR-R	GGCGGAATTCtcaGTGATGGTGATGGTGATGGGATCCgttaacttgatccaaagctctg
SacII-M-mHIF1av1	Ttaaccgcggtggtatggagggcgccggcggcgagaacgagaag
SacII-E-mHIF1av1	ttaaccgcggtggtGAGGGCGCCGGCGGCGAGAACGAGAAG
SacII-R-mHIF1av1	ttaaccgcggtggtagaGAGGGCGCCGGCGGCGAGAACGAGAAG
SacII-G-mHIF1av1	ttaaccgcggtggtGGCGCCGGCGGCGAGAACGAGAAG
mHIF1av1-BamH1-R	ttaaggatcccgttaacttgatccaaagctctgagtaattc
Hif1A P402-F	cactctgctggctGcagctgccggcga
Hif1A P402-R	tcgccggcagctgCagccagcagagtg
Hif1A P577-F	ggagatgctggctGGctatatcccaatg
Hif1A P577-R	cattgggatatagCCagccagcatctcc
Ub Xho1-F	TATATCTCGAGatgcaaattttcgtcaagactttg
Hif1 BamH1-R	TTAAGGATCCcgttaacttgatccaaagctctgagtaat
NgoMIV-Kozak-F	taatgccggccggatcagccgccaccatg
SalI-GFP-R	atatgtcgacggcgcgccttacttgtacagctcgtccatg
C23-25-F	cctccttccagtctggctactccaagaacaagttgggcagtcgc
C23-25-R	gttcttggagtagccagactggaaggaggtctggccctc
HIF1A qPCR-F	CCACAGGACAGTACAGGATG
HIF1A qPCR-R	TCAAGTCGTGCTGAATAATACC
Gapdh qPCR-F	CTGAGGACCAGGTTGTCTCC
Gapdh qPCR-R	GCCTCTCTTGCTCAGTGTCC
mEPO qPCR_F	CATCTGCGACAGTCGAGTTCTG
mEPO qPCR_R	CACAACCCATCGTGACATTTTC
PFKFB3 qPCR_F	TTGTGGCCTCCAACATCAT

PFKFB3 qPCR_R	TCCATGGCTTCTGCTGAGTT
18s rRNA qPCR_F	CGGCTACCACATCCAAGGAA
18s rRNA qPCR_R	GCTGGAATTACCGCGGCT
β-actin (ACTB)_qPCR_F	– CAGCTGAGAGGGAAATCGTG
β-actin (ACTB)_qPCR_R	CGTTGCCAATAGTGATGACC
HK1-qPCR_F	GCGTGGACGGGACGCTCTAC
HK1_qPCR_R	CCTTCACTGTTTGGTGCATGATTC
Serpine_qPCR_F	AGGATCGAGGTAAACGAGAGC
Serpine_qPCR_R	GCGGGCTGAGATGACAAA
mVEGFA_Ori_qPCR_F	CTGCTGTAACGATGAAGCCCTG
mVEGFA_Ori_qPCR_R	GCTGTAGGAAGCTCATCTCTCC
h_Hif1_qPCR_F	CGCATCTTGATAAGGCCTC
h_Hif1_qPCR_R	AATCACCAGCATCCAGAAG
hHK1_qPCR_F	CTGCTGGTGAAAATCCGTAGTGG
hHK1_qPCR_R	GTCCAAGAAGTCAGAGATGCAGG
hPFKFB3_F	GGCAGGAGAATGTGCTGGTCAT
hPFKFB3_R	CATAAGCGACAGGCGTCAGTTTC
hACTB_qPCR_F	CACCATTGGCAATGAGCGGTTC
hACTB_qPCR_R	AGGTCTTTGCGGATGTCCACGT
HPRT1_qPCR_F	CATTATGCTGAGGATTTGGAAAGG
HPRT1_qPCR_R	CTTGAGCACACAGAGGGCTACA